Available online at www.sciencedirect.com
ScienceDirect
Journal of Nuclear Materials 374 (2008) 390–402
journal of nuclear materials
www.elsevier.com/locate/jnucmat

Modelling deuterium release during thermal desorption of D^+-irradiated tungsten

M. Poon, A.A. Haasz *, J.W. Davis

University of Toronto Institute for Aerospace Studies, Toronto, ON, Canada M3H 5T6

Received 14 December 2006; accepted 4 September 2007

Abstract

Thermal desorption profiles were modelled based on SIMS measurements of implantation profiles and using the multi-trap diffusion code TMAP7 [G.R. Longhurst, TMAP7: Tritium Migration Analysis Program, User Manual, Idaho National Laboratory, INEEL/EXT-04-02352 (2004)]. The thermal desorption profiles were the result of 500 eV/D^+ irradiations on single crystal tungsten at 300 and 500 K to fluences of 10^{22}–10^{24} D^+/m^2. SIMS depth profiling was performed after irradiation to obtain the distribution of trapped D within the top 60 nm of the surface. Thermal desorption spectroscopy (TDS) was performed subsequently to obtain desorption profiles and to extract the total trapped D inventory. The SIMS profiles were calibrated to give D concentrations. To account for the total trapped D inventory measured by TDS, SIMS depth distributions were used in the near-surface (surface to 30 nm), NRA measurements [V.Kh. Alimov, J. Roth, M. Mayer, J. Nucl. Mater. 337–339 (2005) 619] were used in the range 1–7 μm, and a linear drop in the D distribution was assumed in the intermediate sub-surface region (~30 nm to 1 μm). Traps were assumed to be saturated so that the D distribution also represented the trap distribution. Three trap energies, 1.07 ± 0.03, 1.34 ± 0.03 and 2.1 ± 0.05 eV were required to model the 520, 640 and 900 K desorption peaks, respectively. The 1.34 and 1.07 eV traps correspond to trapping of a first and second D atom at a vacancy, respectively, while the 2.1 eV trap corresponds to atomic D trapping at a void. A fourth trap energy of 0.65 eV was used to fit the 400 K desorption peak observed by Quastel et al. [A.D. Quastel, J.W. Davis, A.A. Haasz, R.G. Macaulay-Newcombe, J. Nucl. Mater. 359 (2006) 8].

PACS: 28.52.Fa; 79.20.Rf; 61.80.Jh; 61.82.Bg

1. Introduction

There is still considerable debate regarding the choice of plasma-facing materials for the next generation of fusion devices such as ITER. Some of the materials being considered are tungsten-based. The primary advantages of tungsten are its ability to tolerate high temperatures and its high threshold for physical sputtering. The use of tungsten in the low ion energy regions of the reactor, such as the divertor, may be a solution to the problems of wall erosion, hydrogen co-deposition, and high levels of wall impurities in the plasma. However, there are also some concerns surrounding the use of tungsten materials in a fusion reactor, e.g., mechanical and thermal toughness, melting, and tritium inventories during operation and after shutdown.

In this paper, we are addressing the possible tritium inventories in tungsten due to energetic ion irradiation. Direct experiments with tritium (^3_1H) are generally difficult and costly, and usually not performed. Instead, experiments are performed using hydrogen (^1_1H) or deuterium (^2_1H), with the observations and trends applied to tritium. Unfortunately, in most cases, experiments fail to reproduce the high flux densities and fluences present in a real fusion device. Despite these limitations in accurately simulating tritium plasma irradiation of tungsten, the information gained by the experiments enables us to identify the processes and mechanisms governing hydrogen and deuterium

* Corresponding author.
E-mail address: tonyhaasz@utias.utoronto.ca (A.A. Haasz).

0022-3115/$ - see front matter © 2007 Elsevier B.V. All rights reserved.
doi:10.1016/j.jnucmat.2007.09.028

trapping. Ultimately, these experimental results will provide the basis for a model to accurately predict the tritium inventory in tungsten under fusion reactor conditions.

There have been numerous attempts to model hydrogen irradiation and release from tungsten using both re-emission and thermal desorption data with varying degrees of success [1–11]. The main difficulty in developing a consistent model stems from the simulation of the hydrogen irradiation process. Irradiation, particularly at high flux and high energy, is a dynamic, non-equilibrium process. It is known that hydrogen irradiation, even at energies below the threshold for displacement damage, is capable of creating bubbles and blisters in tungsten, e.g., [12–15]. At such energies, the irradiation can also enhance vacancy transport [16]. These voids and vacancies are known to trap hydrogen [17–19]. Unfortunately, modelling codes such as TMAP [20], PIDAT [21] and DIFFUSE [22] are unable to account for the movement, creation and evolution of these vacancy-type traps. As a result, unrealistically high trap concentrations (>0.10 traps/W [3,8]) must be assumed in the unirradiated specimen in order to obtain the required fits. For the purposes of this paper, we will circumvent the difficulties of modelling the irradiation process by starting our simulations after irradiation. Thus, we will only be modelling the thermal desorption portion of the experiments.

Compared to the irradiation process, modelling the thermal desorption of trapped inventories is considerably simpler. In our experiments (e.g., [23–25]), the long *delay time* (several days) between the end of irradiation and start of desorption allows the tungsten-hydrogen system to reach an equilibrium state prior to heating. During heating (~5 K/s), the system is considered to be in quasi-equilibrium with the interstitial hydrogen obeying Sieverts' law. The assumption of equilibrium also ensures the absence of super-saturation of empty vacancies that can lead to vacancy clustering and void creation upon heating. Vacancies containing hydrogen are stable and will not contribute to clustering until the hydrogen becomes de-trapped, allowing the vacancy to be mobile. The mobility of vacancies during thermal desorption is limited to vacancy diffusion; vacancies are generally considered mobile only above ¼ of the melting temperature [26], i.e., above ~900 K for tungsten. Modelling codes such as TMAP [20,27] are well-suited to the thermal desorption process with static traps.

2. Experiment

Several single crystal tungsten (SCW) specimens were used to produce the experimental data [23–25,28] used for modelling the thermal release of trapped hydrogen. These specimens were produced by the State Institute of Rare Metals (Moscow). The quoted purity was 99.9 at.% with the main impurities being H (0.02 at.%), C (0.05 at.%) and O (0.05 at.%). The orientation of the single crystal surface was within 10° of the [0 0 1] plane [23]. Prior to each irradiation, the specimens were mechanically and electrochemically polished, removing several μm of the surface. This polishing treatment was required to remove any effects of previous irradiations [13,23]. After polishing, the specimens were annealed at 1775 K for 30 min to help remove any residue from the electro-polish and reduce the impurity and dislocation content in the bulk. This anneal temperature was also sufficient to break up any vacancy clusters [19].

All irradiations were performed in the single-beam ion accelerator facility at the University of Toronto Institute for Aerospace Studies (UTIAS). A beam of 1.5 keV D_3^+ ions (500 eV/D^+), at normal incidence to the specimen, was used in all experiments. The range of flux densities and fluences were $\sim 5\times10^{19}$–10^{20} D^+/m^2s and 10^{22}–10^{24} D^+/m^2, respectively. A ceramic heater clamped to the back of the specimen allowed for irradiations at 500 K.

Secondary ion mass spectroscopy (SIMS) was performed at the Department of Chemical Engineering, University of Toronto, several days after irradiation. This time delay allowed the release of D in solution and weakly trapped D [28]. The size of the sputter spot created by SIMS (0.04 mm^2) was small compared to the irradiated area (3.14 mm^2) and thus did not significantly affect the results of the subsequent thermal desorption.

Several days after the SIMS analysis, thermal desorption spectroscopy (TDS) was performed at UTIAS. For the TDS data presented here, the specimens were heated from 300 to 1775 K at ~5 K/s and the released D_2, HD, and D_2O were monitored in the residual gas by a quadrupole mass spectrometer (QMS). The QMS signals were calibrated during each desorption with a D_2 leak bottle. The relative H_2/D_2 sensitivity was checked periodically using H_2 and D_2 leaks. The sensitivity of HD was assumed to be the average of the H_2 and D_2 sensitivities, and the sensitivity of D_2O was assumed to be the same as for H_2O; see for example [23].

3. Model development

The recently updated TMAP7 (Tritium Migration and Analysis Program, version 7) code [27] provided by Dr. Glen Longhurst was the backbone of our simulations. For details of the code and governing equations, the reader is referred to [27]. The most powerful attribute of the TMAP7 code is its ability to model multiple trap energies within the same computational segment. Here we assume up to three different trap energies; a fourth trap energy will be considered for a special case of *weakly trapped deuterium* in Section 5.3. The assumption of three trap energies is supported by the thermal desorption data [23–25,28] that show at least three clearly visible peaks, *albeit* not all peaks occur under all experimental conditions. Erents [29] has suggested three types of damage configuration with different activation energies for release. A trap energy of about 1.4 eV has been associated with deuterium trapping at vacancies in tungsten [10,30] and this trap energy has been

widely used in other models [2,4,6,7,10,11,17,18,30]. (In the present paper, the trap energy refers to the binding energy plus the Frauenfelder activation energy of 0.39 eV [31]). A lower energy trap (<1.4 eV) has been associated with the trapping of a second deuterium atom at an existing vacancy-deuterium complex [18,29]. Finally, we assume a high trap energy (>1.4 eV), associated with the dissociation and release of deuterium decorating a void [17]. Note that we do not assume any trap energies associated with weak trapping at impurities or dislocations [10,32]. The long post-irradiation time delays prior to SIMS and TDS were sufficient to release the weakly trapped deuterium [10,28,32–34], as well as deuterium in solution [3,4,32,35].

3.1. Deuterium transport in tungsten

To describe the transport of deuterium in tungsten, we will be using the diffusion coefficient determined by Frauenfelder [31]. Compared to other experimental determinations of the diffusion coefficient, Frauenfelder performed the experiments at temperatures high enough (1120–2080 K) to nullify the effects of trapping. Thus, the Frauenfelder diffusion coefficient gives a true measure of interstitial hydrogen diffusion and agrees within a factor of two with Zener and Wert's theory of interstitial atomic diffusion [36]. In theory [36], the diffusion exponential pre-factor varies inversely with the square root of the mass of the interstitial atom. Accordingly, we have corrected the diffusion coefficient to reflect deuterium diffusion,

$$D_0 = 2.9 \times 10^{-7} \exp(-0.39\ \mathrm{eV}/kT)\ \mathrm{m}^2/\mathrm{s}, \quad (1)$$

where k is the Boltzmann constant and T is the temperature.

TMAP7 [27] allows for two different mechanisms of dissociation and recombination: (i) for dissociation/recombination processes that are sufficiently close to equilibrium that a solution law, Sieverts' or Henry's law, applies (rate-dependent boundary condition); and (ii) rate-limited chemisorption for the adsorption and release of molecules from a surface not in equilibrium with the surrounding gas (surface-dependent boundary condition). In the thermal desorption data being considered for the present model, the specimens were exposed to air for at least 20 min and one can assume an oxygen covered tungsten surface prior to thermal desorption, which was performed in a separate vacuum chamber; see experimental setup [13,37]. Research by Eleveld et al. [30] has shown that surface adsorption of oxygen on tungsten can be used to overcome the problem of deuterium surface re-trapping, such that de-trapping of deuterium from sub-surface defects will not be influenced by surface effects. Therefore, to accurately model the thermal desorption data, a rate-dependent (*ratedep*) boundary will be assumed. The *ratedep* boundary condition requires values for both the recombination and dissociation coefficients. The derived values for the recombination coefficient, K_r, of hydrogen on tungsten vary by over six orders of magnitude [1–3,8], not including the assumption of infinite recombination [4–6]. We have chosen to use the value by Anderl et al. [1],

$$K_r = 3.2 \times 10^{-15} \exp(-1.16\ \mathrm{eV}/kT)\ \mathrm{m}^4/\mathrm{s}, \quad (2)$$

derived from deuterium permeation measurements through tungsten foils. This value was chosen because it is intermediate relative to the other recombination coefficients and is based on experimental evidence rather than strictly modelling considerations. The dissociation coefficient was calculated assuming equilibrium conditions with a net surface flux of deuterium atoms, J_D, of zero,

$$J_D = K_d P - K_r C_D^2 = 0, \quad (3)$$

and Sieverts law,

$$C_D = S\sqrt{P}, \quad (4)$$

where K_d is the dissociation coefficient, C_D the atomic concentration of D, S the solubility coefficient, and P the pressure.

Using the Frauenfelder solubility coefficient for hydrogen in tungsten [31],

$$S = 9.3 \times 10^{-3} \exp(-1.04\ \mathrm{eV}/kT)(\mathrm{D/W})\ \mathrm{atm}^{1/2}, \quad (5)$$

we get the dissociation coefficient,

$$K_d = K_r S^2 = 1.09 \times 10^{34} \exp(-3.24\ \mathrm{eV}/kT). \quad (6)$$

3.2. Deuterium concentration profiles

The final parameters to consider are the trap distribution and the deuterium concentration profile resulting from the irradiation. We will allow ourselves only a limited amount of freedom with these parameters. The implanted deuterium concentration profile was determined by the SIMS depth profiling and the total trapped inventory was measured by TDS.

The first step was to calibrate the SIMS profiles from a raw count to give an atomic concentration. Two sets of SIMS depth profiles and associated TDS D release profiles obtained for irradiations at 500 K were used in the calibration; see Fig. 1. These data sets were used because the TDS profiles were simple, showing a single desorption peak without a long desorption tail at high temperatures. The single peak suggests only one trap mechanism and the sharp edge on the high temperature side of the peak suggests that the trapped deuterium is confined within a limited range, i.e., deuterium is not trapped to large depths in the specimen. Based on the SIMS profile, we assume that all of the trapped deuterium is located in the near-surface peak, within 50 nm of the surface. This assumption is at least partially supported by the results of Alimov et al. who have seen the trapped D atom concentration to be localized within the near-surface for irradiation of tungsten at 650 K [34] – albeit our results were obtained at 500 K. (We note that in the case of Alimov et al. [34] the D^+ energy was 6 keV and the corresponding D atom concentrations for 300 K and 650 K extended to ~2 μm and

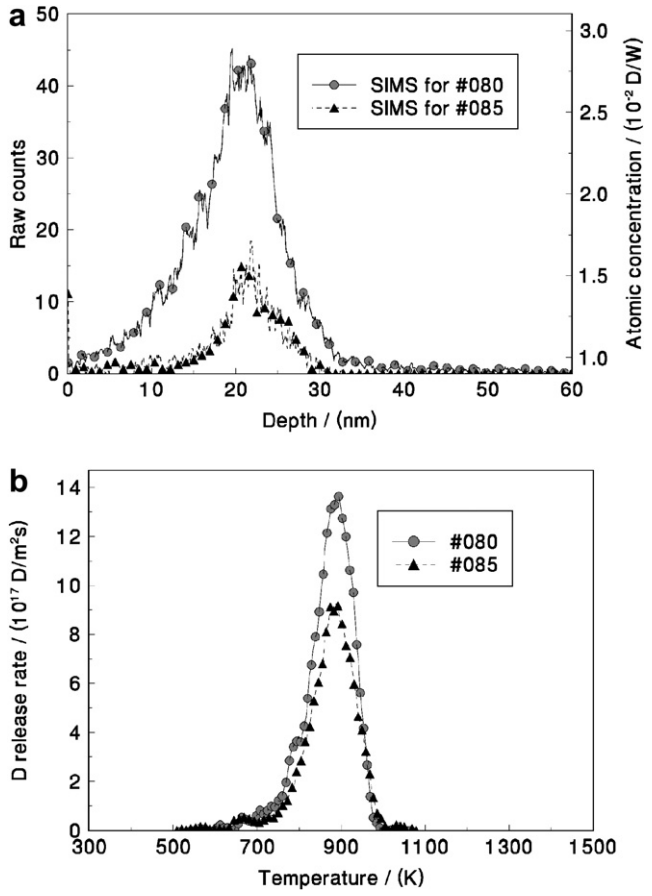

Fig. 1. SIMS and TDS profiles for calibration of SIMS signals for SCW specimens (#080 and #085) irradiated with 500 eV D^+ to 10^{24} D^+/m^2 at 500 K [24,25]. (a) SIMS depth profiles given in terms of the raw counts and calibrated atomic concentration. (b) TDS profiles corresponding to each SIMS profile in (a). The heating rates during thermal desorption were 4.3 K/s and 5.2 K/s for specimens #080 and #085, respectively.

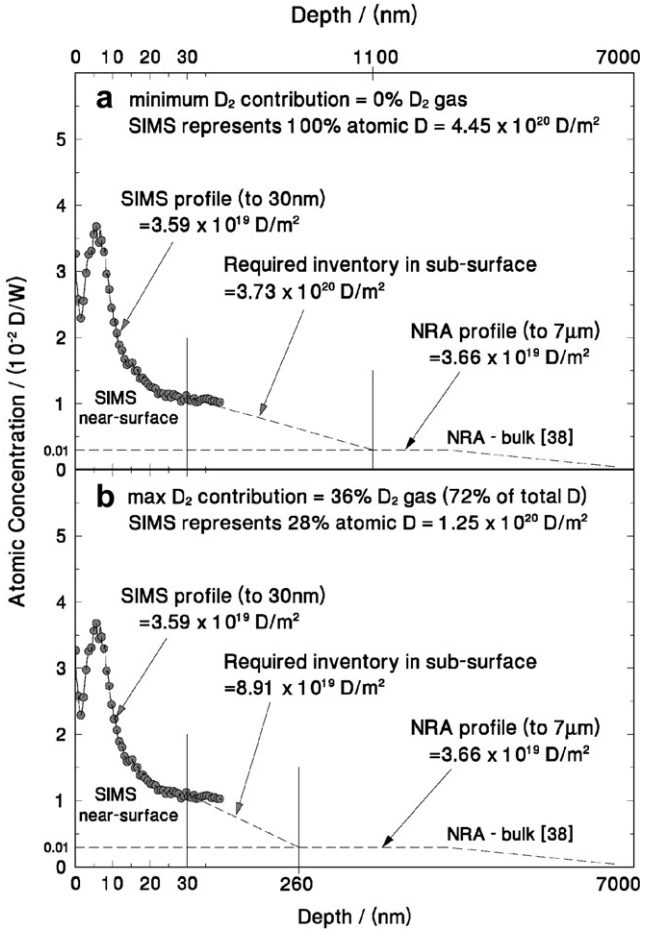

Fig. 2. Example of SIMS depth profile and assumed distributions constructed to account for the uncertainty in the amount of undetected D_2 gas released during SIMS from specimen #076 irradiated with 500 eV D^+ at 300 K [25]. (a) assuming no D_2 gas release during SIMS so the SIMS concentrations are representative of the total inventory, and (b) assuming maximum D_2 gas release (as determined by the Gaussian fits) that is not detected during SIMS so that the SIMS concentrations represent only a fraction of the total inventory.

~500 nm, respectively.) Integration of this peak yields the trapped inventory (D/m^2). To convert the raw counts, R, to an atomic concentration, C, we assume a conversion factor, κ (atomic concentration/count), and a detection threshold, T_d (atomic concentration). Thus the *trapped inventory* can be written as:

$$\text{trapped inventory} = \int_0^{50\text{ nm}} C\,dx = \int_0^{50\text{ nm}} (\kappa R + T_d)\,dx. \tag{7}$$

The detection threshold, T_d, represents the minimum D concentration detectable by SIMS. This is a reasonable assumption given the finite sensitivity of a real device and that only a small fraction of the deuterium atoms released during SIMS are actually detected. A conversion factor of $\kappa = 5.05 \times 10^{-4}$ (D/W)/count and a minimum detection threshold of $T_d = 8.4 \times 10^{-3}$ D/W were derived.

The resulting concentrations of trapped D are consistent with the concentrations observed by Alimov et al. [34]. This conversion factor was also applied to the SIMS data obtained for irradiations at 300 K. However, for the 300 K cases, integration of the near-surface SIMS peak is insufficient to account for the total trapped inventory measured by TDS. Unlike D irradiations of single crystal tungsten at elevated temperatures, irradiations at 300 K result in D trapping at depths well beyond the ion range [12,14,34,37–39]. The SIMS apparatus used here was limited to depths of ~80 nm, and thus for the 300 K irradiations, the SIMS depth profiles were unable to account for all of the trapped deuterium. In such cases, we assume a linear drop in the trapped D distribution, starting at 30 nm and extending into the sub-surface (i.e., 30 nm to 1 μm). Beyond the sub-surface, the NRA data of Alimov et al. [38] are used to estimate the trapped D concentrations in the bulk (1–7 μm).

There is another complication associated with the 300 K irradiation cases: Alimov et al. [34], using combined SIMS/RGA depth profiling, observed both atomic D and molecu-

lar D_2 gas release from specimens irradiated at 300 K; no D_2 release was observed for the 650 K irradiations [34]. In the present SIMS depth profiling, only sputtered ions could be detected so quantitative values for molecular D_2 release were not obtained. Depending on the amount of D_2 gas released, the detected deuterium ions in the SIMS profile may represent only a fraction of the total trapped inventory. Although a firm assessment of the D_2 release could not be obtained, an upper estimate can be made. Using this estimate, two distributions of trapped D can be constructed. One assumes that the SIMS profile represents all of the trapped D (no release of D_2 during SIMS), and the other assumes that a maximum fraction of D is released as D_2 gas so the SIMS profile represents only a fraction of the total trapped inventory. Determination of this maximum fraction of D_2 release will be described below. For both profiles, a linear decreasing depth distribution is assumed in the sub-surface region (30 nm to 1 μm); see Fig. 2.

Many of the TDS profiles are not simple single peaks, but rather, peaks with shoulders or double peaks that suggest the presence of multiple trap energies. In addition to the total inventory and distribution of trapped D, it is necessary to determine the inventory and distribution of trapped D corresponding to each trap energy. The inventory for each trap energy was relatively easy to estimate from the TDS profiles. As a first approximation, the TDS profiles were fitted by a series of Gaussian functions (Fig. 3). The contribution of each desorption peak to the total D inventory was given by the relative areas of the Gaussian functions. To estimate the concentration distributions for the different trap energies, the nature of the traps associated with the various desorption temperatures is considered. Deuterium is known to be trapped in tungsten at impurities, dislocations, vacancies and voids. From the present TDS profiles, desorption temperatures of 900 K, 640 K, and 520 K were observed. In addition, Quastel et al. [28] observed an additional low temperature desorption peak at 400 K. The task is to link the trap mechanisms with the observed desorption temperatures.

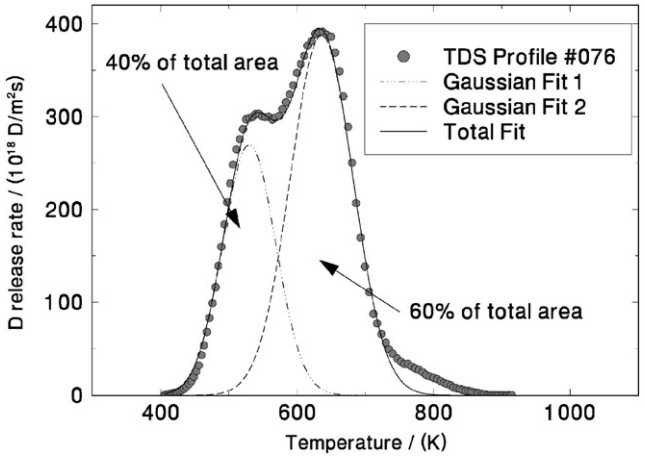

Fig. 3. Example of multiple peaked TDS profile with Gaussian fits to determine the relative amounts of D associated with each desorption peak. The total fit is the sum of Gaussian fits 1 and 2. SCW specimen #076 irradiated with 500 eV D^+ to 10^{24} D^+/m^2 at 300 K [25].

(i) *Deuterium release near 900 K is a result of de-trapping from D decorated voids* [17,19]. The strongest trap mechanism for D in tungsten is having a D atom bound on the inner surface of a void, with trap energies of 1.8–2.1 eV [17]. The clustering of vacancies into voids will only occur in regions of high vacancy concentration or high interstitial concentration, where void formation leads to the greatest decrease in free energy. During irradiation, the highest vacancy and interstitial concentrations will be within the implantation zone. However, vacancy clustering may not be confined to the implantation zone, as evidenced by blister formation at μm depths [13,14,39]. In the SCW experiments used for the present modelling, the 900 K TDS release peak was only observed with the 500 K irradiations and in each case, just the single peak was seen. The corresponding SIMS depth profiles showed D trapping limited to the first 40 nm; see Fig. 1. Our present SIMS depth profiling was limited to the first 80 nm, so there was uncertainty whether or not a deeper D concentration peak existed, as observed by Alimov et al. [39] with the 200 eV D^+ plasma irradiation of SCW at 463 K and 533 K. Comparisons with the SIMS/RGA depth profiling by Alimov et al. [34] of 6 keV D^+ ion irradiation of SCW at 650 K will help us assess the extent of D trapping beyond our SIMS range. Alimov et al. [34] profiled to a depth of 500 nm with no indications of a second D peak indicative of surface blisters. It was also noted that the mean ion range for 6 keV D^+ was ~50 nm and D trapping was held within ten mean ion ranges. One would expect that a much lower energy (500 eV D^+) ion irradiation would have a much shallower D depth profile (i.e., <500 nm). Comparing mean ion ranges for 500 eV D^+ on SCW (~8 nm) and 6 keV D^+ (~50 nm), and assuming similar depth profile to ion range ratios for the two energies, one would expect the trapped D profile to be limited to about 80 nm. Thus, for irradiations at 500 K, the trapped D depth distribution was completely determined by the SIMS depth profiles. Note that comparisons were not made against the 200 eV D^+ plasma irradiations at 463 K and 533 K [39] because although the energies were similar, high flux plasma irradiations can create effects not observed with lower ion flux irradiations.

(ii) *The release peak near 640 K is ascribed to de-trapping from vacancies* [17–19,30,34] *and may occur in the near-surface as well as throughout the tungsten bulk.* Trapping of atomic D at vacancies [30] and as molecular D_2 in highly pressurized voids [17] have the trap energy of about 1.4 eV, corresponding to release temperatures of 500–650 K. However, associated with D_2 gas trapped in voids is atomic D adsorbed on the void

walls. Adsorption of atomic D inside a cavity is a precursor for D_2 gas within the cavity and thus evidence of D-decorated voids must accompany the presence of D_2 gas. None of our TDS results give indications of D-decorated voids (900 K desorption peak) when the 500–650 K desorption peaks are present. Therefore, we must conclude that deuterium is not trapped as D_2 gas in voids. The 640 K desorption peak must be due to vacancies. Vacancies are point defects inherent in any solid and will occur throughout the material. Energetic ion irradiation can greatly increase the local vacancy concentration by displacing the lattice atoms through collisions.

(iii) *The peak/shoulder near 520 K is assumed to be desorption of the second D trapped at a vacancy* [18,29]. This secondary vacancy trap leads to the formation of the D_2V complex. Thus, the inventory associated with the 520 K desorption represents the aforementioned maximum amount of D_2 that could be released during the SIMS analysis, and thus not accounted for in the SIMS profiles. As with the primary vacancy-D trap (at 640 K), D from the secondary trap can be found in both the near-surface and the bulk, but obviously, a vacancy-D complex must already be present and the concentration cannot be greater than that of the primary vacancy-D complexes.

Both the 520 K and 640 K desorption peaks were observed for irradiations at 300 K – but not present for 500 K irradiations. Because of the possibility of unaccounted D_2 gas release from the D_2V complex during SIMS, two different D concentration distributions for the primary and secondary vacancy traps were modelled. For one model, no D_2 gas was assumed so that the SIMS profile was representative of the total trapped content. In this case, the relative sizes of the Gaussian fits helped determine the local concentration. For example, if the local concentration is 0.01 D/W and the Gaussian fits show 60% of the total area to be associated with the 640 K (primary) peak and 40% with the 520 K (secondary) peak, then 0.006 D/W will be attributed to the primary trap and 0.004 D/W will be attributed to the secondary trap. In the other concentration distribution, it is assumed that all of the D_2V complexes are released as D_2 gas and not detected by SIMS. In this case, the SIMS depth profile would represent only the D trapped in the primary vacancy traps with the secondary trap empty. This time, in the case of a 60:40 ratio between 640 K and 520 K Gaussian fits, the SIMS profile would represent only 20% of the total trapped inventory since 80% (40% from the secondary trap and 40% from the primary trap of the D_2V complex) would have been released as D_2 gas. It is assumed that the distribution of D trapped in the D_2V complexes mirrors the atomic D distribution given by the SIMS results. These two distributions represent the extreme limits regarding the possibility of D_2 release during SIMS. An example of the two distributions is shown for a case of 300 K irradiation in Fig. 2.

3.3. Trap distributions

Now that we have interpreted the SIMS and TDS data to obtain the distributions of trapped deuterium, we consider the trap distributions. Previous models [1–8,11] have used uniform trap distributions to track deuterium in tungsten from the start of irradiation through to thermal desorption. While such assumptions may be perfectly valid descriptions of the tungsten material prior to irradiation, they greatly oversimplify the trap concentrations after irradiation. The problem is that these models do not allow the creation, motion and evolution of traps during irradiation. Since we are confining our modelling to the thermal desorption stage, we can circumvent the difficulties associated with trap evolution during irradiation by using the SIMS depth profiles after irradiation as a basis for the trap distributions in the near-surface region. The main assumption here is that the traps are all full so that the trap concentration distribution is identical to the D concentration profiles deduced from the SIMS profiles and TDS data. From permeation transient data, Anderl et al. [1] expected a high fraction of trap sites to be filled. The assumption of a full or saturated trap distribution is not unreasonable, particularly for higher fluence implantations. Consider a 10^{24} D^+/m^2 irradiation with a trapped inventory of 5×10^{20} D/m^2. This implies that only one in every 2000 implanted deuterium is trapped. It seems unlikely that a significant number of traps within the deuterium trapping range could still be empty. The TDS observations by Quastel et al. [28] provide direct evidence of vacancy trap saturation following irradiation. Quastel et al. observed desorption from lower energy traps at 400 K in addition to the higher energy vacancy traps desorbing at 600 K and 500 K. If there were a significant population of vacancy traps available, D released from the lower energy traps would be re-trapped in the higher energy vacancy traps and there would be no 400 K TDS peak. In other words, the existence of a 400 K desorption peak implies that the higher energy traps are expected to be filled during irradiation. TMAP simulations confirm re-trapping to vacant higher energy traps (see Section 5.2).

However, due to the procedure used for TDS, there is a situation where empty trap sites are considered. Prior to the linear heating ramp for TDS, the vacuum chamber was mildly baked to ~373 K for 1–2 h to quickly achieve background pressures on the order of 10^{-6} Pa. As shown by Quastel et al. [28], this mild bake was capable of releasing a significant fraction of the D held in the secondary vacancy trap (520 K peak), and therefore, in order to accurately reproduce our TDS profiles, we will assume that a fraction of the secondary vacancy traps will be empty; the primary vacancy traps (640 K peak) will still be assumed to be saturated. The fraction of empty secondary vacancy traps is determined by the *primary:secondary* ratio obtained from the Gaussian fits to the TDS profiles. For example, for a 60:40 ratio of *primary:secondary* vacancy traps, two-thirds of the vacancies will have two trapped

D atoms. One-third of the vacancies will only have one D trapped, so for these vacancies, the secondary trap is considered empty. However, this estimate may be an oversimplification because from minimum potential energy considerations, not all vacancies may be capable of trapping two D atoms. It may not be energetically favourable to have neighbouring vacancies each with two trapped D atoms. Thus, there may be a maximum fraction of DV complexes that can trap a second D atom. The present TDS data give a maximum ratio of 67% secondary-to-primary traps, occurring with the 3×10^{23} D^+/m^2 irradiation. At this irradiation fluence, the retained vs. incident curve reaches a plateau [23] which may indicate saturation of all the trap sites. If this were the case, then the maximum fraction of DV complexes capable of trapping a second D atom may be close to 67%. For our modelling, we will use a 70% fraction. Therefore, for a 60:40 ratio of primary to secondary traps, with trap concentrations of 0.6 and 0.4 at.%, respectively, the maximum *available* secondary trap concentration is 0.42 at.%, so the secondary trap occupancy will be ~95%.

4. Results

4.1. Irradiations at 500 K

SIMS depth distributions and TDS profiles were obtained for two single crystal tungsten specimens irradiated to 10^{24} D^+/m^2 at 500 K [24,25]. The TDS profiles and TMAP7 fits are shown in Fig. 4; the corresponding SIMS depth distributions presented in Fig. 1(a) show all of the deuterium to be trapped within the first 40 nm of the surface. We note that the mean ion range, R, for 500 eV D^+ on tungsten is ~8 nm, as calculated by TRVMC [40]. Thus, all of the deuterium was trapped within 5 mean ion ranges. This trap distribution is consistent with the observations by Alimov et al. [34] where 70% of the trapped deuterium was contained within three mean ion ranges for 6 keV D^+ ion irradiations at 650 K. The latest results by Alimov and Roth [39] for single crystal tungsten exposed to a high flux 200 eV D^+ plasma at 463 K and 533 K with NRA depth profiles show a large near-surface (<100 nm) peak in the D concentration. However, under these high flux plasma conditions, an additional peak was seen at depths of about 1 μm that may be associated with the presence of surface blisters. No surface blistering was observed with our results so the second D concentration peak would not be expected and all the deuterium could be accounted for within the near-surface peak. For our cases, saturated 2.1 ± 0.05 eV traps gave the best fits to the thermal desorption profiles for 500 eV/D^+ irradiations at 500 K. This trap energy is associated with de-trapping of atomic deuterium from voids [17,19]. High concentrations of D atoms in the near-surface layer have been observed by Alimov et al. [34] after D^+ ion irradiations at 650 K on single crystal tungsten and have also been attributed to D adsorbed on microvoid walls.

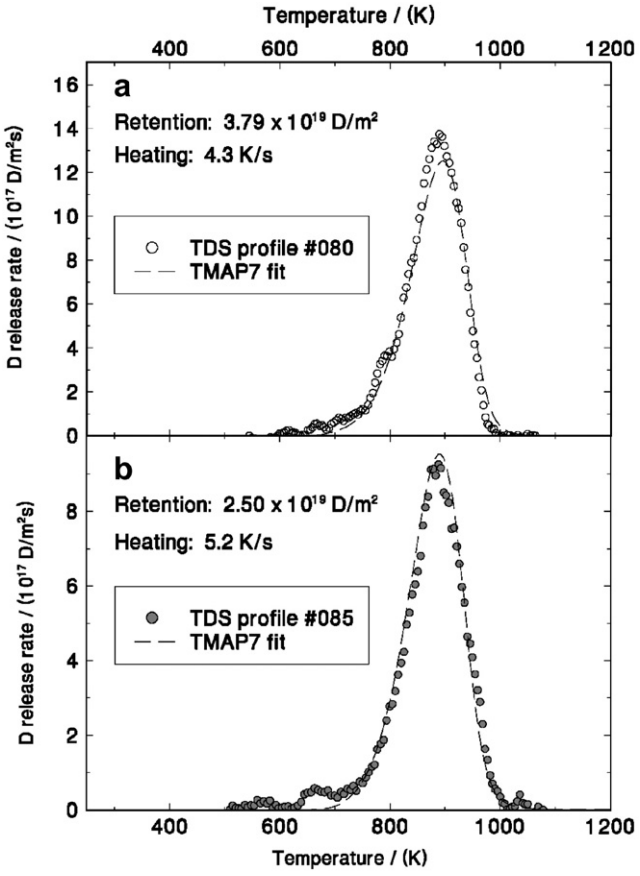

Fig. 4. TDS profiles and TMAP7 fits for thermal desorption of SCW irradiated with 500 eV D^+ to 10^{24} D^+/m^2 at 500 K [24,25]. (a) Specimen #080 and (b) Specimen #085. The main difference between the two cases is the heating rate.

4.1.1. Attempts to fit TDS profiles using a single 1.4 eV energy trap

We have also attempted to fit the above TDS profiles obtained for 500 eV/D^+ irradiations at 500 K using 1.4 eV traps only. Venhaus and Causey [6] have suggested that a single trap energy of 1.4 eV is sufficient to describe the trapping behaviour of hydrogen in tungsten. There are two ways that a lower energy trap can exhibit the same peak desorption temperature as a higher energy trap. (i) In one situation, the deuterium may be physically deep inside the specimen so that there is a diffusion lag time between de-trapping and surface release. (ii) In the second situation, there may be a large fraction of empty traps allowing the deuterium atoms to be re-trapped many times before desorbing from the surface.

(i) *Assuming that D is deep inside the specimen:* In the above discussions we have provided evidence that for our 500 eV D^+ ion irradiations at 500 K, all of the trapped D is contained within the top 50 nm. However, it would be useful to assess whether or not deeply trapped D in 1.4 eV traps could re-create a desorption peak at 900 K. Consider the SIMS/

RGA depth profile for deuterium by Alimov et al. [34] for 6 keV D^+ ion irradiation to 8×10^{22} D^+/m^2 at 650 K on SCW (Fig. 5(a)). In this depth profile, trapped D is found to depths of 500 nm – an order of magnitude deeper than our present results. TMAP modelling of the deep distribution with saturated 2.1 eV traps produces a desorption peak at 950 K (similar to our 500 eV/D^+ case with saturated 2.1 eV traps), whereas a model with saturated 1.4 eV traps produces a desorption peak at 650 K; see Fig. 5(b). Unfortunately, a thermal desorption curve for this irradiation condition was not available for comparison. A trap energy of 1.95 eV is required to produce a desorption peak at 900 K – note that this trap energy is still within the range (1.8–2.1 eV) for trapping of D on the inner surfaces of voids [17,19]. As shown by the modelling results, physically deeper 1.4 eV traps are unable to re-create a desorption peak at 900 K.

(ii) *Assuming the existence of many empty traps:* Here we assume that there may be a large fraction of empty traps such that deuterium atoms may be re-trapped many times before desorbing from the surface. While it is possible to fit the TDS data using 1.4 eV traps, the trap concentration becomes unrealistically high. In order to achieve a 900 K desorption peak with 1.4 eV traps, the fraction of filled traps must drop to <0.02%, requiring trap concentrations of up to

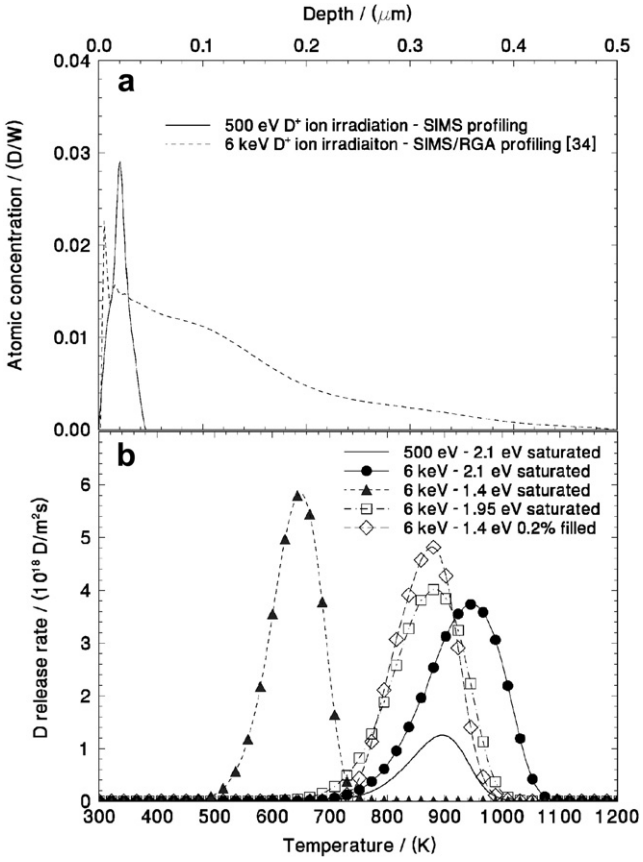

Fig. 5. (a) Deuterium depth distributions obtained by SIMS profiling of SCW irradiated with 500 eV D^+ at 500 K (present study) and by Alimov et al. using SIMS/RGA for SCW irradiated with 6 keV D^+ at 650 K [34]. (b) TMAP7 modelled fits for different trap energies and trap occupancies corresponding to the deuterium depth profiles in (a).

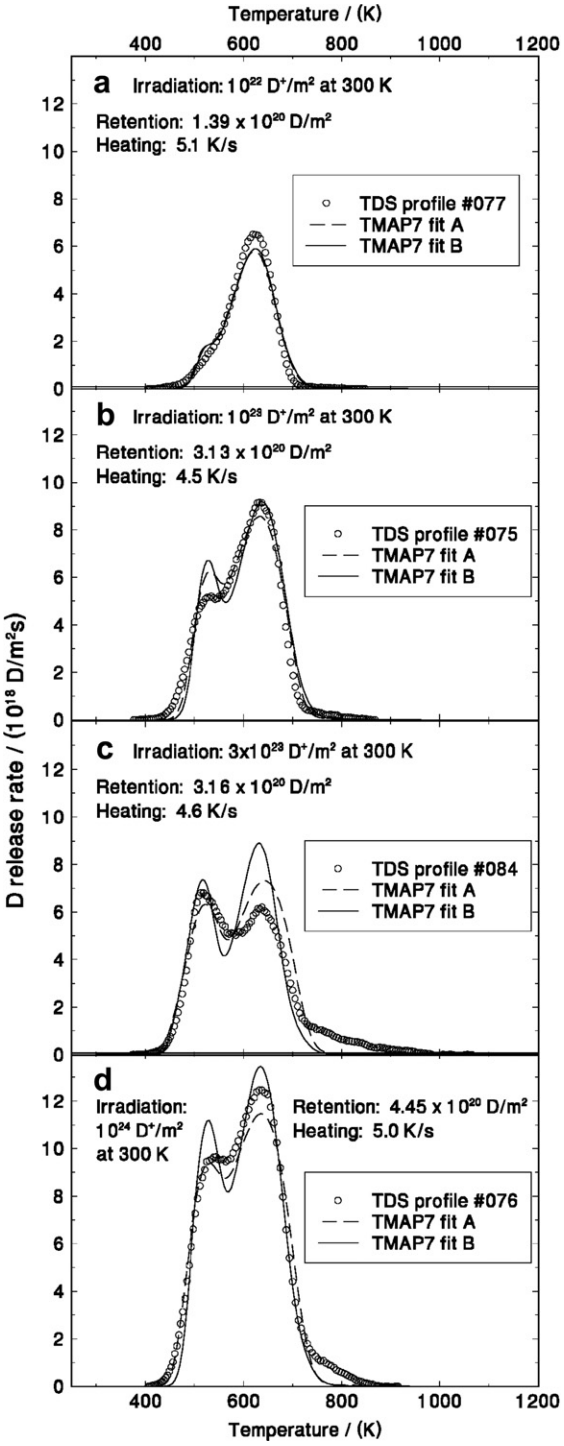

Fig. 6. TDS profiles and TMAP7 fits for thermal desorption of SCW irradiated with 500 eV D^+ to various fluences at 300 K [24,25]. TMAP7 fit A uses trap distributions assuming no D_2 gas release during SIMS, and TMAP7 fit B uses trap distributions assuming maximum D_2 gas release that is not detected during SIMS.

140 traps/W. To put this into perspective, to create the necessary number of trap sites, one would require a trap creation rate of 0.2 traps/D^+, which is unrealistically high for 500 eV D^+ irradiation of tungsten.

We will also check if 1.4 eV traps used in combination with deeper trapping and reduced trap occupancy can result in a 900 K desorption peak. For a deep distribution, we will again use the Alimov et al. [34] SIMS/RGA depth profile of 6 keV D^+ ion irradiation on SCW at 650 K (Fig. 5(a)). In order to re-create the required 900 K desorption peak using 1.4 eV traps, a very low occupancy ratio of 0.2% (0.002 D/trap) is required; see Fig. 5(b). On the contrary, researchers modelling hydrogen re-emission from tungsten have found that a high fraction of occupied trap sites was required [1,9]. To achieve this low occupancy ratio, trap concentrations of up to 7 traps/W were required. This appears to be an unrealistically high concentration, considering that modelling 800 MeV proton irradiation of tungsten only required a trap density of 0.075 traps/W [7]. With such extreme conditions required for the 1.4 eV fitting to work, we must conclude that for our data, the 1.4 eV trap cannot be used to model the 900 K TDS release peak. Also, as noted in Section 3.3, the existence of a 400 K desorption peak implies that the higher energy traps are expected to be filled during 500 eV D^+ irradiations at 500 K [28].

4.2. Irradiations at 300 K

SIMS depth distributions and TDS profiles were obtained for several irradiation fluences at 300 K. The TDS profiles [24,25] and corresponding TMAP7 fits are given in Fig. 6. In each case, integration of the near-surface SIMS deuterium distribution was insufficient to account for the total amount of D released during TDS. Two trap distributions were considered to account for the possibility that D_2 gas was released during SIMS but not detected; see Section 3.2 (iii). In each case, a linear decrease in D atom concentration was assumed beyond 30 nm and NRA depth profiling was used to estimate the bulk concentrations to 7 μm [38]; see Fig. 2.

Modelling the TDS profiles for 300 K irradiations proved to be more difficult than the 500 K irradiations because several of the thermal desorption profiles exhibited peaks at 640 and 520 K. Two trap energies were required to fit the profiles; they were assumed to correspond to trapping of a first (640 K: primary) and second (520 K: secondary) deuterium at a vacancy. The relative concentration of each trap was based on the Gaussian fits to the TDS profiles, with small adjustments made to obtain the best fits. The trap energies were also adjusted according to each thermal desorption profile. This fitting was done for each trap distribution. The characteristics of the trap distributions and parameters for the best fits are given in Table 1. When fitting the trap distributions assuming no D_2 release during SIMS ('A' distributions), the best overall trap energies were 1.32 ± 0.02 and 1.06 ± 0.03 eV for the primary and secondary vacancy traps, respectively. The trap distributions assuming maximum D_2 release ('B' distributions) were best fit with 1.36 ± 0.02 eV (primary) and 1.08 ± 0.03 eV (secondary) trap energies overall. In all cases, the fitted trap energies from the A distributions were lower than those from the B distributions. Also, the resulting TDS profiles from the B distributions tended to have narrower and more pronounced desorption peaks.

Since the A and B distributions represent the extreme cases, the real distribution must lie somewhere between these extremes, and correspondingly, the trap energies should lie within the range of fitted values. An estimate to the primary vacancy trap will be taken to be 1.34 ± 0.03 eV, and for the secondary vacancy trap, 1.07 ± 0.03 eV. The ratio of the population of primary to secondary traps (see Table 1) was observed to generally decrease with fluence, with the exception of the 10^{24} D^+/m^2 irradiation which showed a slight increase over the 3×10^{23} D^+/m^2 irradiation, but was still lower than the 10^{23} D^+/m^2 irradiation. This general trend is expected since the primary trap must first be occupied before the secondary trap can exist and as the local concentration of primary traps becomes saturated, the secondary traps begin to fill.

Table 1
Deuterium trap distribution and TMAP7 fitting parameters for simulating thermal desorption of D from single crystal tungsten after irradiation to various fluences at 300 K [24,25]

Irradiation fluence (D^+/m^2)	Sample ID	Primary: secondary ratio	Assumed distribution A or B (depth) (nm)	Fitted primary vacancy trap energy (eV)	Fitted secondary vacancy trap energy (eV)
10^{22}	#077	88:12	A (370)	1.33	1.03
			B (280)	1.34	1.05
10^{23}	#075	70:30	A (830)	1.30	1.06
			B (310)	1.34	1.08
3×10^{23}	#084	60:40	A (930)	1.34	1.08
			B (130)	1.37	1.10
10^{24}	#076	64:36	A (1130)	1.30	1.06
			B (260)	1.35	1.10

Distribution 'A' assumes no D_2 release during SIMS and distribution 'B' assumes a maximum D_2 release during SIMS (equal to the secondary fraction) that is not detected.

However, this ratio does not reach unity, but rather, appears to hold at around a 60:40 *(primary:secondary)* ratio above 3×10^{23} D^+/m^2 irradiations. This coincides with the flattening of the retention versus incident fluence curve for 300 K irradiation on single crystal tungsten [23].

5. Discussion

5.1. Nature of traps derived from modelling

We have shown that thermal desorption profiles can be successfully modelled from measured post-irradiation depth distributions using the TMAP7 code and trap energies of 1.07 ± 0.03, 1.34 ± 0.03 and 2.1 ± 0.05 eV. However, it is also important to establish the nature of these traps. Most researchers, e.g., [17,25,30,34], agree that the higher trap energy of 2.1 eV can be attributed to trapping of atomic hydrogen on the inner surfaces of voids. Many researchers, e.g., [18,30], also agree that the 1.4 eV (1.34 eV in our results) trap energy is due to atomic hydrogen at vacancies. Anderl et al. [1] have also suggested that dislocations may be responsible for the 1.4 eV trap, but admit that this trap energy appears high for a dislocation type trap. Using 6 keV D^+ irradiations on single crystal tungsten at room temperature, Alimov et al. [34] detected D_2 molecules and micro-voids within the implantation zone and suggest that the 1.4 eV traps result from D_2 gas inside voids. The 6 keV D^+ energy is well above the threshold for displacement damage [40] and capable of creating vacancy defects. It is reasonable to assume that a vacancy super-saturation condition may exist within the implantation zone, leading to the creation of voids. However, in our experiments, the ion energy is well below the threshold for displacement damage, so void creation appears unlikely. Low ion energies below the threshold for displacement damage have been found to create surface blisters on single crystal tungsten, but only when using a high flux plasma source for irradiation [39,41]. In these cases, it is believed that the high D^+ flux creates a local D super-saturation in the tungsten material, leading to plastic deformation and void creation. The D^+ flux from our ion accelerator is 1–2 orders of magnitude lower than that of a plasma device and appears to be incapable of creating blisters in single crystal tungsten. In fact, from our 300 K irradiations (Fig. 6), trapping of D_2 gas in voids can be ruled out because of the absence of the 900 K desorption peak associated with atomic D bound on the inner surface of voids – as is seen in Fig. 1 for 500 K irradiations.

In order for D_2 gas to be released from a void during TDS, the D_2 molecule must first dissociate at the void surface and adsorption of atomic D on the surface of the void cannot be avoided; thus the 2.1 eV trap energy (corresponding to a 900 K release peak) must also be present with the trapping of D_2 gas. However, there is a possibility that D_2 molecules can be detected by the SIMS/RGA method of Alimov et al. [34] without the existence of D_2 gas in cavities. As explained earlier, the release of D_2 molecules during SIMS sputtering could be caused by two deuterium atoms trapped at a single vacancy, creating a D_2V complex and the detected D_2 gas could simply be the remnant of a D_2V complex. Thus, as discussed above, for the 300 K irradiations two trap distributions were modelled to take this possibility into account. With our irradiation conditions, our modelled 1.34 eV (near the nominal 1.4 eV) trap energy is due to D trapping at vacancies.

5.2. Effect of variation of model parameters

5.2.1. Effect of additional empty traps

While obtaining modelling fits to the thermal desorption data, several trends were observed. It was found that an abundance of empty, lower energy traps had no effect on the TDS profiles. In fitting the 500 K results (Fig. 4), a uniform distribution of empty vacancy traps, simulating the inherent vacancy content, was added to the saturated distribution of 2.1 eV traps. The addition of these empty, lower energy traps even up to 0.01 traps/W, had no effect on the simulated thermal desorption profile. This result allows us to perform accurate simulations without having to include an empty distribution of lower energy traps to account for weak trapping at dislocations and impurities (earlier, it was noted that the present TDS results were devoid of weakly trapped deuterium). Conversely, adding an abundance of empty, higher energy traps will significantly affect the thermal desorption profiles. Deuterium released from lower energy traps will be re-trapped in the higher energy traps. In fact, if the abundance of empty, higher energy traps is greater than the amount of D held in the lower energy traps, nearly all of the released D will be re-trapped and the resulting TDS profile will only show the effects of the higher energy trap (all evidence of the existence of the lower energy traps will be lost).

To illustrate the effects of empty trap concentrations, the simulated TMAP7 desorption profile #076 (10^{24} D^+/m^2 at 300 K, fit A in Fig. 6(d)) will be used as the reference. In one case, an empty concentration of higher energy (2.1 eV) traps was added to the simulation. The empty 2.1 eV trap distribution was equivalent to the trap concentration used for simulating the thermal desorption profile #085 in Fig. 1(a). It should be noted that the concentration of empty 2.1 eV traps added was only 2.24×10^{19} traps/m^2, equivalent to 5% of the total trap inventory of 4.45×10^{20} traps/m^2. This case would correspond to the situation of D_2 gas trapped in voids without atomic D adsorbed on the cavity walls. It is clear that even with a small 5% addition of empty, higher energy traps, D released from the 1.07 eV traps (520 K peak) is re-trapped at the 2.1 eV trap sites, resulting in the obvious release peak at 900 K (Fig. 7). This is additional support that one cannot have D_2 gas de-trapping from voids with a trap energy of ~1.4 eV without evidence of atomic D de-trapping from void surfaces at 2.1 eV.

In the second case, an empty concentration of lower energy (0.65 eV) traps was added to the simulation. Here,

a constant distribution of 2.5×10^{-4} traps/W was added to a depth of 20 μm, giving an empty trap inventory of 3.2×10^{20} traps/m^2, or 72% of the original trap inventory. Fig. 7 shows that even the addition of a larger number of empty, lower energy traps has no effect on the thermal desorption of D from higher energy traps.

5.2.2. Effect of trap energy, trap occupancy, trap location and TDS heating rate

During the fitting process, the temperature of the simulated thermal release peaks was found to be dependent upon three factors – the trap energy, the occupancy of the traps, and the physical depth of the traps from the surface. A higher trap energy, lower occupancy fraction, and physically deeper trap location could all increase the temperature of the release peaks. With the same trap energy, one could always produce a higher release temperature by lowering the trap occupancy and pushing the traps deeper into the bulk (it was possible to move the single vacancy-trap release peak from 640 K to 900 K using the same 1.34 eV trap energy). Technically, one could also create a lower release peak by increasing the occupancy and having traps near the surface, however, one is severely limited by trap saturation and the physical limit of the surface (it is not possible to move the 2.1 eV release peak from 900 K to 640 K). It was found that the width of the TDS profiles gave an indication of the physical spread of the trap distribution. Narrow thermal release peaks indicated very localized trap distributions and broad peaks signified broad trap distributions. The shallower and more localized trap distributions assumed with maximum D_2 gas release during SIMS resulted in higher trap energies and sharper desorption peaks compared to the deeper and broader trap distributions associated with the assumption of no D_2 gas release during SIMS. Also, significant deviations in the linearity of the heating rate (greater than 25% change) could create artificially high desorption peak heights during periods of higher heating, and reduce peak heights during periods of reduced heating. All of the experimental heating ramps were quite linear (±5%), so non-linear heating effects were not an issue here.

5.2.3. Effect of recombination coefficient

The shapes of the simulated profiles were found to change noticeably with the recombination coefficient (Fig. 8). For comparison purposes, the TMAP7 (#076 fit B) simulated profile for 10^{24} D$^+$/m^2 irradiation at 300 K (Fig. 6(d)), using the nominal recombination coefficient (Eq. (2)) taken from Anderl et al. [1], will be considered as the reference profile. Decreasing the recombination coefficient tended to translate the simulated thermal desorption profiles to higher temperatures – in effect delaying release from the surface, and enhancing the size of the higher temperature peak. Increasing the recombination coefficient did the exact opposite. Upon de-trapping, surface release of D was fast, allowing D release to be detected at lower temperatures accompanied by shifting of the desorption peaks to lower temperatures. Also with increased recombination the desorption peaks appeared to broaden, thus reducing the depth of the valley between the peaks. (Note that with a 10^4 increase of K_r, the 'lower' temperature TDS peak is lost within the 'higher' temperature peak.) Increasing surface recombination above the value measured by Anderl et al. [1] to broaden the peaks may be a solution to reduce the depth of the valleys with the TMAP7 simulations seen in Fig. 6. Increasing surface recombination would also require higher trap energies to counteract the peak shift and may put the modelled trap energies corresponding to the 640

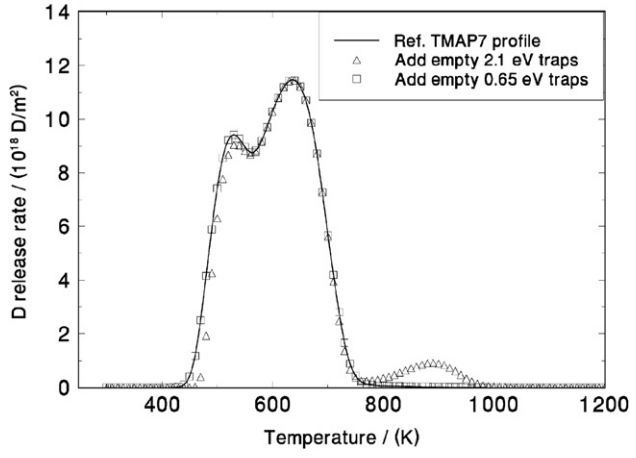

Fig. 7. TMAP7 simulations show the effect of adding concentrations of empty traps. The reference TMAP7 profile for specimen #076 from Fig. 5(d) (dashed line – fit A) is shown here for comparison purposes. The trap inventory in the reference profile is 4.45×10^{20} traps/m^2. The effect of adding empty 2.1 eV traps (2.25×10^{19} traps/m^2) is shown by the open triangles and the effect of adding empty 0.65 eV traps (3.2×10^{20} traps/m^2) is shown by open squares.

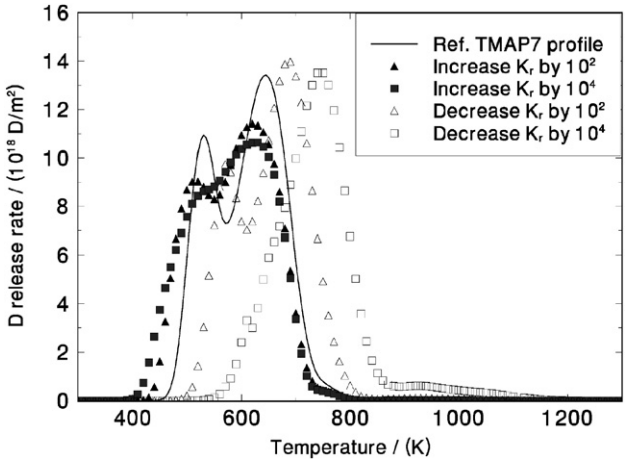

Fig. 8. TMAP7 simulations for different recombination coefficient (K_r) values. The reference TMAP7 profile for specimen #076 from Fig. 5(d) (solid line – fit B) is shown here for comparison purposes; it was based on the recombination coefficient (Eq. (2)) measured by Anderl et al. [1]. The effects of increasing K_r are shown by filled symbols and decreasing K_r by open symbols.

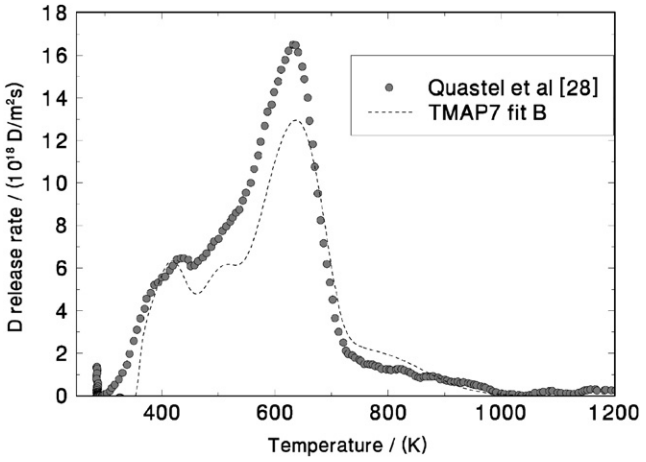

Fig. 9. Experimental TDS profile and TMAP7 modelling for run #15 by Quastel et al. [28] where thermal desorption was performed 20 min after 500 eV D^+ irradiation on SCW to 10^{23} D^+/m^2 at 300 K. Three trap energies were used in the fit: 0.65, 1.1, and 1.37 eV.

and 520 K desorption peaks closer to those reported in the literature [2,5–7,10,11,17,18,30]. Increasing the surface recombination by two orders of magnitude above the value by Anderl et al. [1], the TDS profile for 10^{24} D^+/m^2 irradiation at 300 K (Fig. 6(d) – #076 Fit B) can be fit with 1.15 eV and 1.40 eV traps, compared to 1.07 eV and 1.34 eV obtained with the Anderl et al. surface recombination coefficient.

5.3. Modelling of weakly trapped deuterium

Using this knowledge, we now undertake to fit a thermal desorption profile that includes weakly trapped deuterium. Thermal desorptions by Quastel et al. [28] could be performed within 20 min after irradiation, thus allowing the release of interstitial and weakly trapped D to be observed. The advantage of using the data by Quastel et al. [28] is that the specimens were identical to the ones in this study and the same irradiation facility was used. The TDS profile to be fitted was irradiated with 500 eV D^+ to 10^{23} D^+/m^2 at room temperature, then desorbed 20 min after irradiation (run #15) [28]. The data presented above were obtained under the same irradiation conditions as [28], but the SIMS and TDS in our case were performed several days after irradiation. It is assumed that the only difference between the thermal desorption data of Quastel et al. and the current set is the presence of weakly trapped deuterium. Therefore, to model the result of [28], the same fitting parameters as obtained for #075 Fit B in Fig. 6(b) will be used, with an additional low-energy trap to account for the 400 K release peak and increased D retention. A trap energy of 0.65 eV with a constant distribution of 2.5×10^{-4} trap/W to a depth of 20 μm (Fig. 9) was found to give a good fit to run #15 by Quastel et al. [28]. This trap energy has been associated with trapping at dislocations [10,32].

6. Summary and conclusion

TMAP7 was used successfully to model thermal desorption of a known distribution of trapped deuterium in single crystal tungsten. Experimental TDS produced D release peaks at 520, 640 and 900 K. Using SIMS (present study) and SIMS/NRA [38] depth profiling to provide the known distributions, TMAP7 modelling yielded corresponding trap energies of 1.07 ± 0.03, 1.34 ± 0.03, and 2.1 ± 0.05 eV, respectively. The present results support the idea of vacancy traps of 1.34 and 1.07 eV for the first and second deuterium trapped at a single vacancy, respectively, and trapping of atomic deuterium on void walls with trap energy of 2.1 eV. Extending the model to include the 400 K desorption peak [28] yielded a shallow trap with 0.65 eV energy.

The next step in building a model for hydrogen trapping in tungsten is to accurately simulate the irradiation process to produce the trap distributions and concentrations observed by depth profiling. Such a model must include trap creation, transport, and evolution in order to best simulate experimental results. A molecular dynamics based model is envisioned where traps are regarded as *particles* in much the same way as a deuterium atom. For vacancy traps, mobility would be determined by vacancy diffusion, with enhanced diffusion during irradiation. Trapping can be treated as a reaction between a D atom and a trap to form an atom-trap complex, which in turn will be regarded as a *particle*. De-trapping would simply be the reverse reaction. Trap evolution, such as vacancy clustering to form voids, could be handled as a reaction between several *vacancy particles* to create a *void particle*. With such a dynamic model, the effects of high fluence, high flux, elevated temperatures, and impurities could be extrapolated to reactor conditions.

Acknowledgments

The funding from the *Natural Sciences and Engineering Research Council* of Canada is greatly appreciated. We express special thanks to Dr Glen R. Longhurst for making the updated version of his TMAP7 code available to us; this code was the primary tool for obtaining the modelling results presented here. We also thank Dr V.Kh. Alimov for providing the SCW material, Peter Brodersen at Surface Interface Ontario, University of Toronto, for performing the SIMS analysis and Charles Perez for his careful work in fabricating many parts of the experimental apparatus.

References

[1] R.A. Anderl, D.F. Holland, G.R. Longhurst, et al., Fusion Tech. 21 (1992) 745.
[2] C. Garcia-Rosales, P. Franzen, H. Plank, et al., J. Nucl. Mater. 233–237 (1996) 803.
[3] P. Franzen, C. Garcia-Rosales, H. Plank, V.Kh. Alimov, J. Nucl. Mater. 241–243 (1997) 1082.
[4] R. Causey, K. Wilson, T. Venhaus, W.R. Wampler, J. Nucl. Mater. 266–269 (1999) 467.

[5] T. Venhaus, R. Causey, R. Doerner, T. Abeln, J. Nucl. Mater. 290–293 (2001) 505.
[6] T.J. Venhaus, R.A. Causey, Fusion Technol. 39 (2001) 868.
[7] B.M. Oliver, T.J. Venhaus, R.A. Causey, et al., J. Nucl. Mater. 307–311 (2002) 1418.
[8] R.G. Macaulay-Newcombe, A.A. Haasz, M. Poon, J.W. Davis, in: A. Hassanein (Ed.), Proceedings of the NATO Advanced Research Workshop on Hydrogen Isotope Recycling in Plasma Facing Materials in Fusion Reactors, NATO Science Series II: Mathematics, Physics and Chemistry, vol. 54, Kluwer Academic Publishers, Dordrecht, 2002, p. 145.
[9] A.A. Pisarev, I.D. Voskresensky, S.I. Porfirev, J. Nucl. Mater. 313–316 (2003) 604.
[10] O.V. Ogorodnikova, J. Roth, M. Mayer, J. Nucl. Mater. 313–316 (2003) 469.
[11] B.M. Oliver, R.A. Causey, S.A. Maloy, J. Nucl. Mater. 329–333 (2004) 977.
[12] F.C. Sze, R.P. Doerner, S. Luckhardt, J. Nucl. Mater. 264 (1999) 89.
[13] A.A. Haasz, M. Poon, J.W. Davis, J. Nucl. Mater. 266–269 (1999) 520.
[14] W. Wang, J. Roth, S. Lindig, C.H. Wu, J. Nucl. Mater. 299 (2001) 124.
[15] M.Y. Ye, H. Kanehara, S. Fukuta, et al., J. Nucl. Mater. 313–316 (2003) 72.
[16] Q. Xu, T. Yoshiie, H.C. Huang, Nucl. Instrum. Meth. Phys. Res. B 206 (2003) 123.
[17] A. van Veen, H.A. Filius, J. De Vries, et al., J. Nucl. Mater. 155–157 (1988) 1113.
[18] J.R. Fransens, M.S. Abd El Keriem, F. Pleiter, J. Phys. Cond. Mat. 3 (1991) 9871.
[19] H. Eleveld, A. van Veen, J. Nucl. Mater. 212–215 (1994) 1421.
[20] G.R. Longhurst, D.F. Holland, J.L. Jones, B.J. Merrill, TMAP4: Tritium Migration Analysis Program, Description and User's Manual, INEL report, EGG-FSP-10315, EG & Idaho Inc. (1992).
[21] W. Moller, Tech. Rep. IPP 9/44 Max-Planck-Institut fur Plasmaphysik, Garching, Germany, 1983.
[22] M.I. Baskes, SAND83-8231, Sandia National Laboratories, Livermore, CA, 1983.
[23] M. Poon, A.A. Haasz, J.W. Davis, R.G. Macaulay-Newcombe, J. Nucl. Mater. 313–316 (2003) 199.
[24] M. Poon, R.G. Macaulay-Newcombe, J.W. Davis, A.A. Haasz, J. Nucl. Mater. 337–339 (2005) 629.
[25] Michael Poon, Deuterium Trapping in Tungsten, PhD Thesis, University of Toronto, 2004.
[26] W. Moller, J. Roth, in: D. Post, R. Behrisch (Eds.), Physics of Plasma-Wall Interactions in Controlled Fusion, NATO ASI Series B, vol. 131, Plenum, New York, London, 1986, p. 439.
[27] G.R. Longhurst, TMAP7: Tritium Migration Analysis Program, User Manual, Idaho National Laboratory, INEEL/EXT-04-02352, 2004.
[28] A.D. Quastel, J.W. Davis, A.A. Haasz, R.G. Macaulay-Newcombe, J. Nucl. Mater. 359 (2006) 8.
[29] S.K. Erents, in: Proceedings of the 8th Symposium on Fusion Technology (SOFT), Utrecht, Netherlands, 1974, p. 895.
[30] H. Eleveld, A. van Veen, J. Nucl. Mater. 191–194 (1992) 433.
[31] R. Frauenfelder, J. Vac. Sci. Technol. 6 (1969) 388.
[32] A.A. Pisarev, A.V. Varava, S.K. Zhdanov, J. Nucl. Mater. 220–222 (1995) 926.
[33] R. Sakamoto, T. Muroga, N. Yoshida, J. Nucl. Mater. 233–237 (1996) 776.
[34] V.Kh. Alimov, K. Ertl, J. Roth, K. Schmid, Phys. Scripta T94 (2001) 34.
[35] V.Kh. Alimov, B.M.U. Scherzer, J. Nucl. Mater. 240 (1996) 75.
[36] C. Wert, C. Zener, Phys. Rev. 76 (1949) 1169.
[37] A.A. Haasz, J.W. Davis, M. Poon, R.G. Macaulay-Newcombe, J. Nucl. Mater. 258–263 (1998) 889.
[38] V.Kh. Alimov, J. Roth, M. Mayer, J. Nucl. Mater. 337–339 (2005) 619.
[39] V.Kh. Alimov, J. Roth, Phys. Scripta T128 (2007) 6.
[40] W. Eckstein, Computer simulation of ion-solid interaction, Springer Series in Materials Science, vol. 10, Springer, Berlin, 1991.
[41] K. Tokunaga, M.J. Baldwin, R.P. Doerner, et al., J. Nucl. Mater. 337–339 (2005) 887.